RESEARCH ARTICLE

Sorption Behaviors of Amorphous Titanium Phosphate Towards Neodymium and Dysprosium

Süleyman İnan[1]*

[1]Ege University, Institute of Nuclear Sciences, Bornova-İzmir, 35100, Türkiye

Abstract: Due to the limited supply of critical metals, their recovery from alternative sources has become a very important issue. In particular, end-of-life magnets contain significant amounts of neodymium (Nd) and dysprosium (Dy) ions and are considered secondary sources. The present study focused on the sorption and separation performance of titanium phosphate for Nd and Dy ions in an aqueous solution. In this regard, amorphous titanium phosphate (am-TiP) was prepared via one-step precipitation. XRD, SEM-EDS, FTIR, and BET analysis were utilized to enlighten the morphological, structural, and surface properties of am-TiP. The uptake of Nd^{3+} and Dy^{3+} ions was examined individually and in multiple element solutions depending on solution pH, contact time, metal concentration, and the presence of Co^{2+} ions. The maximum uptake capacity was 40.16 mg/g at pH 6 for Nd^{3+} and 26.95 mg/g at pH 4 for Dy^{3+}. Am-TiP has been observed to exhibit selectivity towards Nd^{3+} and Dy^{3+} ions in solutions containing Co^{2+} ions. The highest desorption yields obtained for Nd^{3+} and Dy^{3+} using 1.0 mol/L HCl were 95.2% and 97.4%, respectively.

1. INTRODUCTION

The group of metals known as Rare Earth (RE) metals, also called the rare-earth elements (REE), is composed of 15 elements that are located between lanthanum and lutetium on the periodic table. RE metals are used in hybrid vehicles, electric vehicles, wind turbines, solar panels, MR machines, and green energy technologies. Many high-end products such as LCD-LED TVs, magnets, rechargeable batteries, digital cameras, and mobile phones include RE metals (1,2).

Neodymium (Nd) has found various applications in different industries. It has been utilized as a coloring agent in glass production and as a component in laser crystals and welding goggles. However, its most widespread usage is in the production of permanent magnets, which are commonly used in wind turbines, electric motors, and computer hard drive spindles. Dysprosium (Dy), another critical rare-earth metal, is currently used for various applications. It is added to neodymium, iron, and

boron (NdFeB) containing magnets as an additive to enhance their high-temperature performance and increase their intrinsic coercivity. Dy is a valuable material in the nuclear sector, where it is commonly used as a radiation shielding component. Additionally, phosphors that contain Dy are employed as radiation detectors in the monitoring of ionizing radiation for clinical and environmental purposes (3).

Nd is a crucial component in the production of neodymium magnets, In addition to Nd and praseodymium (Pr), terbium (Tb) and Dy are essential constituents of Nd magnets, as they enhance their intrinsic coercivity. Nd magnets can contain up to 9% Dy by weight of the total magnet. Both the U.S. DOE and the European Commission have classified Dy and Nd as "critical materials" due to their crucial role in technology and the challenges in their supply (4).

The demand for RE metals is growing with the development industry. In this context, in addition

to primary sources, end-of-life magnets are considered as an alternative source for Nd and Dy supply. NdFeB magnets are a prominent type of magnet known for their high content of RE elements. These magnets typically contain around 31-32% of RE elements, which includes 21-31% of Nd and Pr, as well as 0-10% of Dy, along with minor amounts of Tb and Gd. Additionally, they can also contain up to 5% of cobalt (Co). After their service life has ended, these magnets can be a valuable source of RE elements (5,6). Recycling RE elements can offer a promising and efficient approach to solving the supply problem and environmental concerns related to primary resources such as mining.

Due to its simplicity and effectiveness, sorption is widely utilized for metal recovery and separation. Various materials have been tested for the sorption of Nd^{3+} and Dy^{3+} such as magnetic iron oxide (7), chitosan-manganese-ferrite beads (8), magnetic nano-hydroxyapatite (9), phosphorous functionalized nanoporous carbon (10), biochar (11), NaOH treated bark powder (12), and functionalized mesoporous silica (13).

The separation and recovery of RE metals have recently attracted attention with the use of tetravalent metal phosphate compounds. Avdibegovic et al. reported the ability of crystalline α-zirconium phosphate to effectively separate scandium (Sc) ions from acidic solutions containing iron (Fe) ions. They were successful in achieving high separation factors for Sc(III) over Fe(III) in hydrochloric acid solutions. This finding highlighted the potential of the material for Sc(III) separation (14). Promising results were obtained by Xu et al. for the recovery of metals individually from the Co, Nd, and Dy-bearing mixed solutions using zirconium phosphates (15,16). Recently, Sentürk and İnan have reported that amorphous tin(IV) phosphate has a selectivity for Nd^{3+} and Dy^{3+} in Co^{2+}-bearing solutions (17).

Although there is a growing demand for alternative materials that can efficiently and selectively separate and recover Nd and Dy from acidic leaching solutions, the reported use of metal(IV) phosphate compounds in this field is scarce. With this study, the potential application of am-TiP in the separation and recovery of Nd^{3+} and Dy^{3+} was investigated for the first time, as displayed in Figure 1.
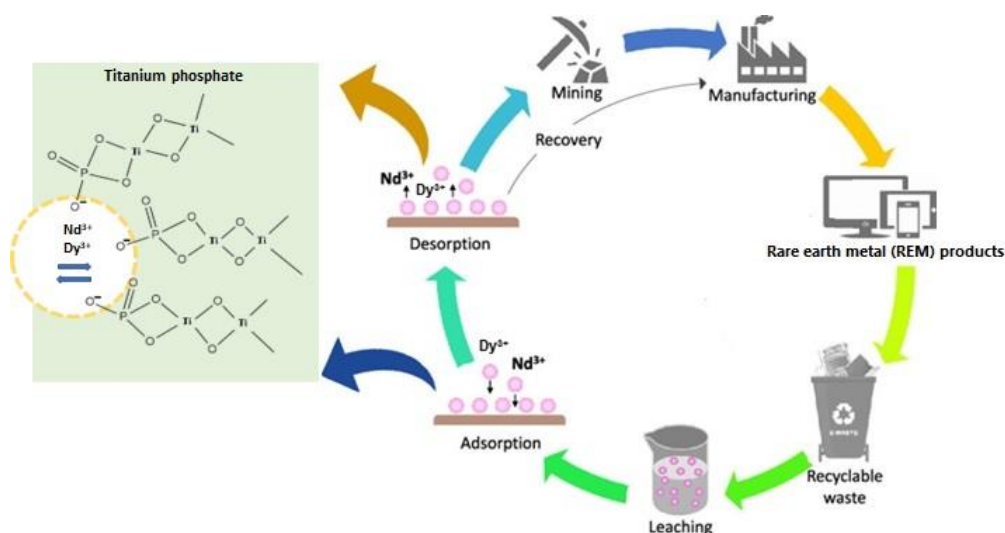
Figure 1: The use of am-TiP for the selective recovery of Nd^{3+} and Dy^{3+} via the sorption-desorption process.

To achieve this goal, am-TiP was prepared and characterized. The impact of process variables on Nd^{3+} and Dy^{3+} uptake was explored. Moreover, the capacity and selectivity of am-TiP were determined in mixed solutions of Nd^{3+}, Dy^{3+}, and Co^{2+} ions. Desorption and reusability studies were carried out to recover Nd^{3+} and Dy^{3+} from loaded am-TiP samples and to evaluate the process from an economic point of view.

2. EXPERIMENTAL SECTION

2.1. Chemicals
Titanium(IV) chloride ($TiCl_4$), sodium hydrogen phosphate (Na_2HPO_4), neodymium(III) nitrate-hexahydrate ($Nd(NO_3)_3 \cdot 6H_2O$), dysprosium(III) nitrate hydrate ($Dy(NO_3)_3 \cdot H_2O$), cobalt(II) nitrate

hexahydrate ($Co(NO_3)_2 \cdot 6H_2O$), nitric acid (HNO_3), sulfuric acid (H_2SO_4), hydrochloric acid (HCl) and ammonia (NH_3) were of analytical grade and supplied from Sigma Aldrich.

2.2. Instrumentation
To determine the crystalline structure, X-ray diffraction (XRD) pattern was recorded in the range of 5°-80° (Thermo Scientific). Chemical bonds and functional groups were identified by Fourier-Transform-Infrared-Spectroscopy (FTIR) in the range of 400-4000 cm^{-1} with an Attenuated Total Reflectance (ATR) apparatus (Perkin Elmer). Surface properties of am-TiP were determined by nitrogen gas adsorption in liquid nitrogen temperature using surface area and porosity analyzer (Micromeritics). The morphology of the surface and

data on the elemental composition was obtained by Scanning Electron Microscope (SEM) equipped with an Energy Dispersive Spectroscopy (EDS) detector (Thermo Scientific Apreo S). The amounts of Nd^{3+}, Dy^{3+}, and Co^{2+} in the solution were analyzed using Inductively Coupled Plasma-Optical Emission Spectroscopy (ICP-OES) (Perkin Elmer).

2.3. Synthesis of Am-TiP
The synthetic method used involved a one-step precipitation process conducted under acidic conditions. Specifically, 0.25 mol/L $TiCl_4$ was added dropwise to 0.25 mol/L Na_2HPO_4 solution under constant stirring at ambient conditions. The resulting mixture was allowed to age overnight, leading to the formation of the white gel-like precipitate.

Following the precipitation step, solid-liquid separation was accomplished through centrifugation at 4000 rpm (Nüve NF 800). The resulting filtrate was then subjected to multiple washings using deionized water and followed by drying at 55 °C for 72 h. The resulting material was ground using a mortar and then sifted using a 120-mesh (0.125 mm) sieve to achieve a grain size suitable for use in sorption tests.

2.4. Design of Experiments
The sorption capacity of am-TiP was evaluated by conducting experimental runs using the batch method at ambient temperature. To perform the experiments, an Erlenmeyer flask was charged with 0.1 g of am-TiP, and then 30 mL of an aqueous phase was introduced. The impact of various factors on the sorption process was investigated through the alteration of selected variables. Solution pH was adjusted to either 0.01-1 mol/L HNO_3 or NH_3. The sorption process was performed by contacting am-TiP with the aqueous phase in a thermostated shaker at 130 rpm. Once the sorption was complete, the suspension was filtered, and 10 mL of filtrate was collected from each sample. The concentration of Nd^{3+} and Dy^{3+} was analyzed using ICP-OES.

The impact of individual factors on the sorption of Nd^{3+} and Dy^{3+} was analyzed in single-element solutions. Initial pH was studied between pH 2 and 6. The contact time varied between 30 to 480 min. Isotherm studies were conducted using solutions containing 10 to 400 mg/L Nd^{3+} and Dy^{3+}.

In multi-element solutions, the influence of metal concentration and pH on the uptake of Nd^{3+}, Dy^{3+}, and Co^{2+} was evaluated by distribution coefficient (K_d) and selectivity coefficient (β). The effect of concentration was examined in equimolar Nd^{3+}, Dy^{3+}, and Co^{2+}-containing solutions over a concentration range of 0.075-1.2 mmol/L at pH 6.

Then, the impact of initial pH was studied in solutions containing Nd^{3+}, Dy^{3+}, and Co^{2+} at an equimolarity of 0.3 mmol/L over a pH range of 2-6.

Sorption characteristics were calculated using the following equations:
Distribution coefficient (K_d)

$$K_d = \frac{(C_i - C_e)}{C_e} \times \frac{V}{m} \, (mL/g)$$

Sorption capacity (q)

$$q = (C_i - C_e) \times \frac{V}{m} \, (mg/g) \quad \text{(Eq. 2)}$$

Selectivity coefficient (β)

$$\beta_{1/2} = \frac{K_{d1}}{K_{d2}} \quad \text{(Eq. 3)}$$

In Eqs. (1-3), K_d is the distribution coefficient (mL/g), β is the selectivity coefficient, K_{d1} and K_{d2} are the distribution coefficients of metal ion 1 and metal ion 2, respectively. C_i and C_e refer to concentration at initial and equilibrium conditions (mg/L), V refers to volume (mL), and m refers to the mass of am-TiP (g).

3. RESULTS AND DISCUSSION

3.1. Characterization of Am-TiP
No significant changes were observed in the FTIR spectra of am-TiP and metal-loaded am-TiP. Therefore, the only spectrum for am-TiP is given in Figure 2a. The presence of the sharp peak at 1035 cm^{-1} indicates the formation of the phosphate structure, as it corresponds to the asymmetric stretching vibration of Ti-O-P. Additionally, the asymmetrical stretching and bending vibrations of O-H are responsible for the peaks observed at 3400 and 1630 cm^{-1} (18).

The surface area and pore structure of am-TiP were evaluated using the BET and Barrett-Joyner-Halenda (BJH) techniques, respectively. BET surface area of am-TiP was measured as 170 m^2/g. BJH analysis showed that the mean pore diameter was 8.2 nm, indicating that the surface of am-TiP is primarily composed of mesopores. The XRD pattern presented in Figure 2b demonstrates that TiP has an amorphous structure. SEM images displayed in Figure 2(c-d) exhibit an irregular morphology and porous structure on the surface. EDS analysis of the surface pattern indicates that it contains 53.62% oxygen, 19.80% phosphorus, and 26.58% titanium by weight, as illustrated in Figure 2e.
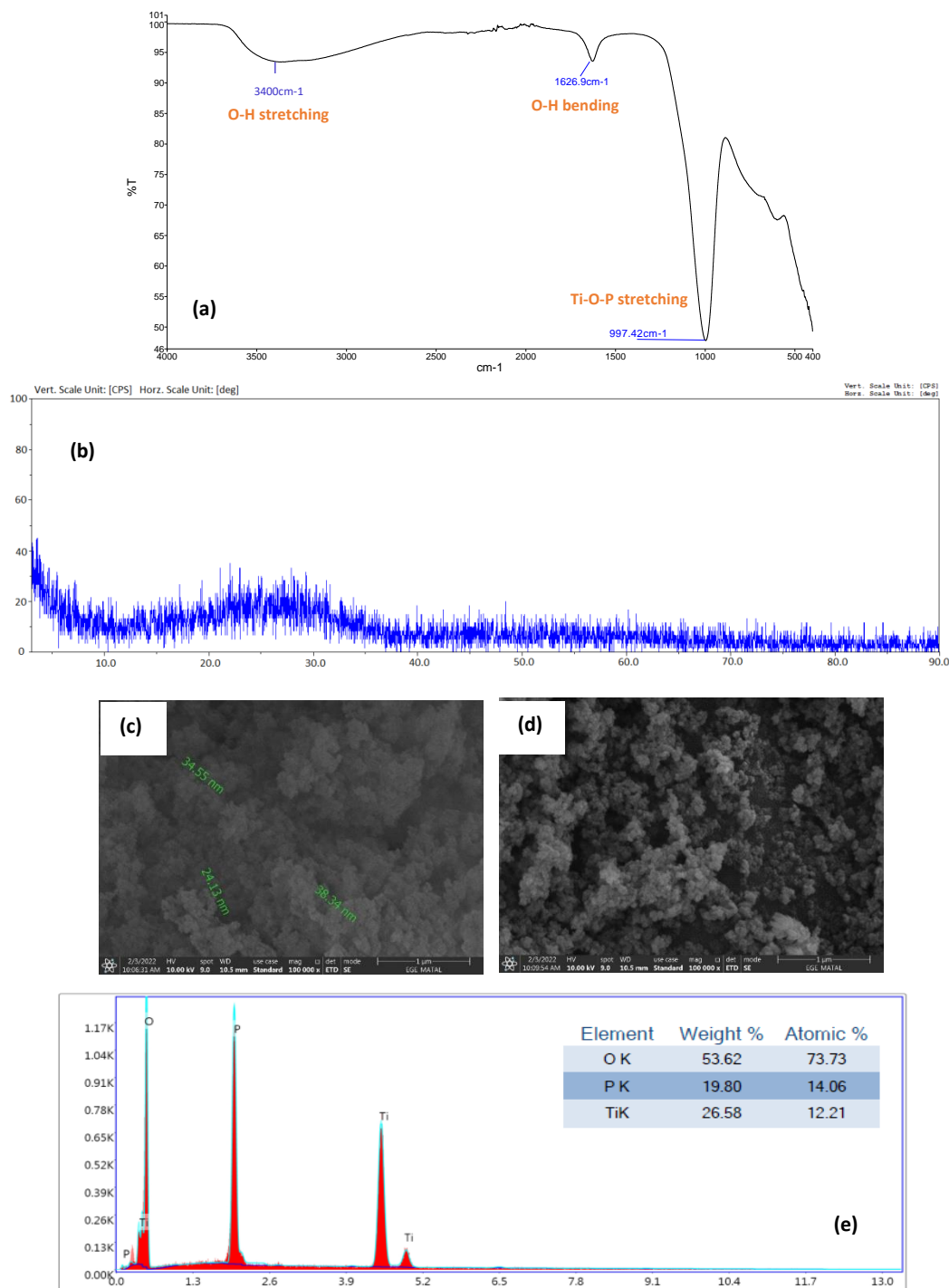
Figure 2: Characterization of am-TiP (a) FTIR spectra, (b) XRD curve, (c-d) SEM images, (e) EDS data.

3.2. Uptake Studies of Nd^{3+} and Dy^{3+} in Single-Element Solutions

3.2.1. The impact of initial pH

The effectiveness of an adsorbent can be affected by the pH level as it can alter the surface charge, ionization degree, and the speciation of the adsorbate. At a pH below the zero-charge point, the surface is likely to carry a positive charge which can lead to a significant decrease in metal adsorption due to the repulsion of metal cations. Additionally, competition occurs between metal ions and H^+ at low pH levels.
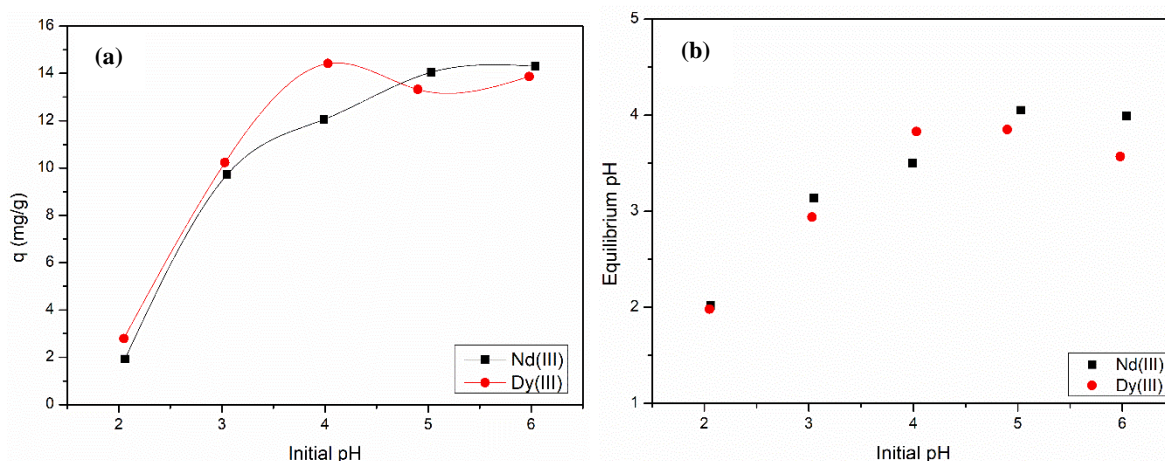
Figure 3: (a) The change in uptake capacity (q) as a function of initial pH, (b) the relationship between equilibrium pH and initial pH.
(Experimental conditions; C_i: 50 mg/L, t: 3 h, T: 25 °C, m_{am-TiP}: 0.1 g, V: 30 mL)

The impact of the initial pH on the sorption was examined in an acidic to neutral medium since leach solutions originating from the hydrometallurgical process have an acidic character. As shown in Figure 3a, increasing the pH from 2 to 5 resulted in a rise in Nd^{3+} adsorption from 1.93 to 14.05 mg/g. However, the rate of increase in adsorption capacity decreased significantly after reaching a maximum and became almost constant. On the other hand, Dy^{3+} uptake sharply increased between pH 2-4 and peaked at 14.42 mg/g at pH 4, followed by a slight decrease in capacity and a tendency to remain constant after pH 4 (Figure 3a). These trends for both RE metals are further confirmed by the plot in Figure 3b.
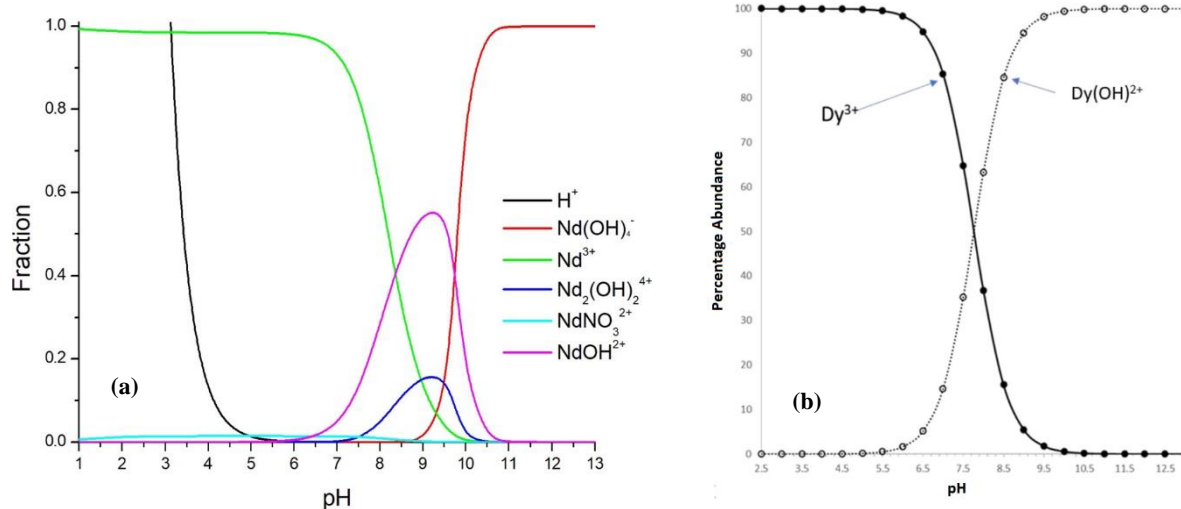
Figure 4: The fraction of (a) neodymium (19) and, (b) dysprosium (20) species as a function of pH.

The highest Nd^{3+} and Dy^{3+} uptake occurred with the range of pH 4.0-6.0 (Figure 3a) due to the reduced effect of hydrogen ions competition, which is confirmed by the speciation of neodymium and dysprosium ions (Figures 4a and 4b). According to Figures 4a and 4b, the trivalent form of Nd (Nd^{3+}) and Dy (Dy^{3+}) was predominant in the studied pH range.

3.2.2. The impact of contact time

The uptake of Nd^{3+} and Dy^{3+} was examined for 15-360 min while fixing the other factors constant. Figure 5 displays the impact of contact time on the sorption capacity of am-TiP for Nd^{3+} and Dy^{3+}. In both cases, there was a slight increase in uptake capacity with the increasing contact time, which then plateaued. For both ions, 60 min was determined to reach the equilibrium conditions, and further investigation was carried out for 60 min.
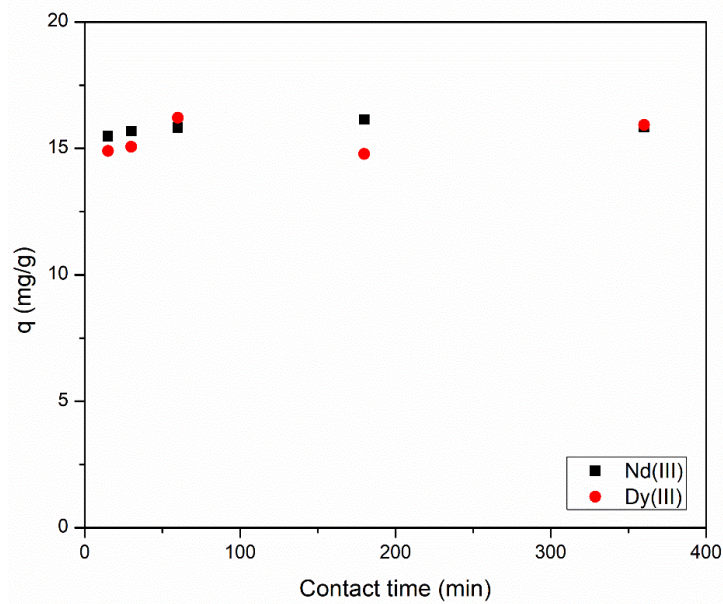
Figure 5: The change in uptake capacity (q) as a function of contact time.
(Experimental conditions: Nd^{3+}, pH: 6; Dy^{3+} pH: 4; C_i: 50 mg/L; T: 25 °C; m_{am-TiP}: 0.1 g; V: 30 mL)

3.2.3. The impact of metal concentration and isotherm studies
The impact of the initial metal concentration was explored by analyzing solutions with concentrations ranging from 10 to 400 mg/L. Figure 6 shows that the uptake of Nd^{3+} and Dy^{3+} increases as the concentration increases, and the maximum saturation capacity for the material has not been reached in the examined range.
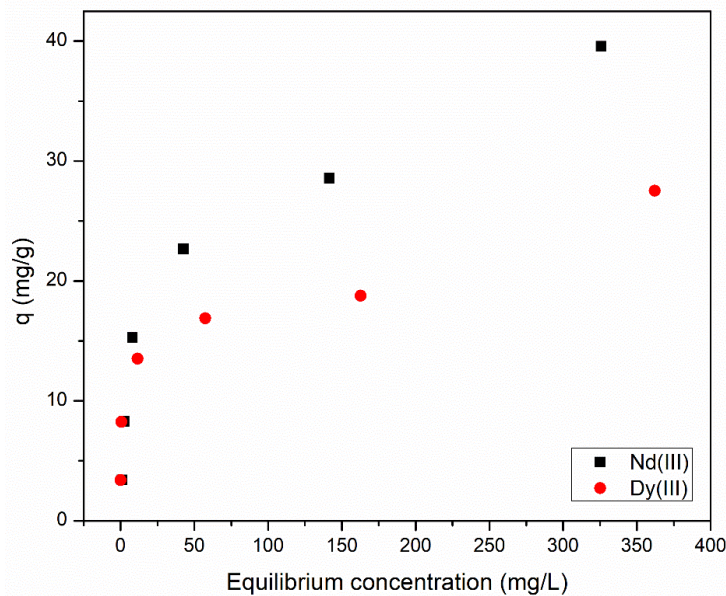
Figure 6: The change in uptake capacity (q) as a function of Nd^{3+} and Dy^{3+} concentrations.
(Experimental conditions; Nd^{3+}, pH: 6; Dy^{3+}, pH: 4; t: 60 min; T: 25 °C; m_{am-TiP}: 0.1 g; V: 30 mL)

The adsorption process is characterized by sorption isotherms. The data obtained from the sorption isotherms were analyzed employing Freundlich and Langmuir models. The Langmuir model assumes that the sorbate molecules form a monolayer on the surface of the sorbent, occupying specific homogeneous sites. The Langmuir equation is commonly linearized as follows (21):

$$\frac{C_e}{q_e} = \frac{C_e}{q_m} + \frac{1}{q_m b} \qquad (Eq.4)$$

where q_e refers to the amount of metal ion sorbed at equilibrium (mg/g), C_e refers to the concentration of a metal ion at equilibrium (mg/L), q_m refers to monolayer sorption capacity (mg/g) and b refers to constant related to the free energy of sorption (L/g). Based on the data presented in Figure 7a and Table 1, it can be concluded that the Langmuir model fits the experimental data quite well for the sorption of both ions. It suggests that sorption on the surface occurs as a monolayer coverage.

118
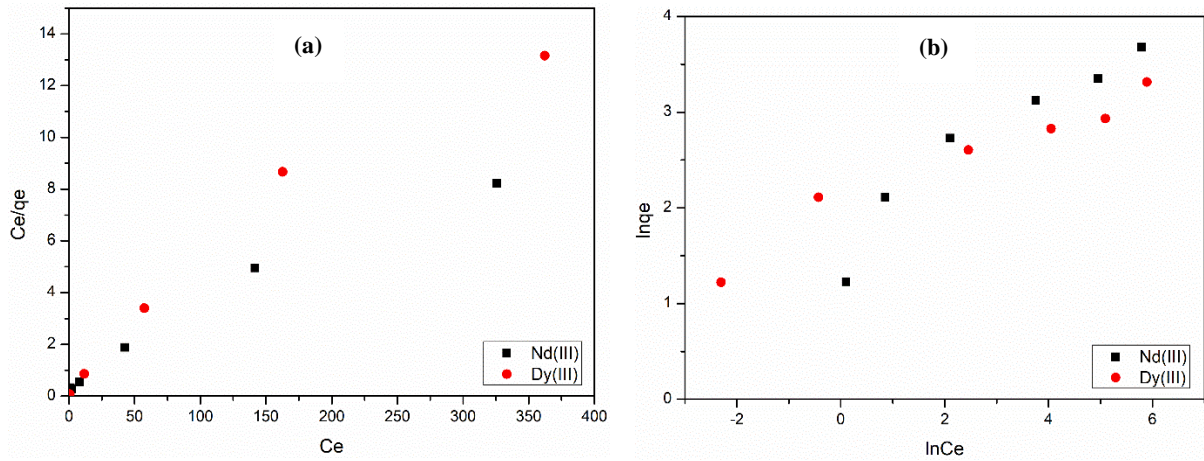
Figure 7: Sorption isotherm curves for Nd^{3+} and Dy^{3+} sorption on am-TiP (a) Langmuir isotherm, (b) Freundlich isotherm.

Table 1: Langmuir and Freundlich isotherm data.

Model	Parameters	Nd^{3+}	Dy^{3+}
Langmuir	q_m (mg/g)	40.16	26.95
	b (L/mg)	0.05	0.05
	R^2	0.976	0.959
Freundlich	1/n	0.38	0.22
	K_f (mol/g)	4.92	7.04
	R^2	0.913	0.946

Table 2: Nd and Dy adsorption performance of various adsorbents.

Sorbent	Rare earth metal	pH	Maximum capacity (mg/g)	Ref
Magnetic iron oxide	Nd^{3+}	8.2	24.88	(7)
Chitosan-manganese-ferrite beads	Nd^{3+}	6	37.87	(8)
Phosphorous functionalized nanoporous carbon	Dy^{3+}	6.6	344.6	(10)
HMVP supported mesoporous silica	Dy^{3+}	5	52.63	(13)
Amorphous tin phosphate (am-SnP)	Nd^{3+} Dy^{3+}	4 3	68.03 58.14	(17)
Expanded vermiculite	Nd^{3+}	3.3	29.57	(19)
Phosphorus functionalized adsorbent	Nd^{3+}	6	160	(23)
Ion-imprinted mesoporous silica	Dy^{3+}	2	22.33	(24)
Oxidized MWCN	Dy^{3+}	4-6	78	(25)
Amorphous titanium phosphate (am-TiP)	Nd^{3+} Dy^{3+}	6 4	40.16 26.95	Present study

The Freundlich model (22) describes multilayer sorption on heterogeneous surfaces, and the equation can be linearized as follows:

$$ln q_e = ln K_f + \frac{1}{n} ln C_e \qquad \text{(Eq. 5)}$$

In Eq. (5), K_f refers to a constant related to the sorption capacity (mol/g) and $1/n$ refers to a parameter dependent on the sorption intensity. The sorption data of Nd^{3+} and Dy^{3+} were found to fit the Freundlich model well, as indicated by the data presented in Table 1 and Figure 7b. K_f and $1/n$ values are calculated to be 4.92 and 0.38 for Nd^{3+} and 7.04 and 0.22 for Dy^{3+}, respectively. The obtained values of $1/n$ between 0 and 1 indicate that the sorption of Nd^{3+} and Dy^{3+} onto am-TiP is favorable under the tested conditions.

Table 2 presents a compilation of prior research on Nd^{3+} and Dy^{3+} sorption. The sorption capacity of am-TiP is competitive with other adsorbents in the slightly acidic-neutral region. Furthermore, its simple synthesis procedure is noteworthy. However, the sorption capacity in more acidic environments can be further improved by modification and functionalization.

3.3. Uptake Studies of Nd^{3+} and Dy^{3+} in Ternary Solutions
Efficient recycling of Nd^{3+} and Dy^{3+} ions require selective separation from leachate solutions in the presence of Co^{2+} ions. Experiments were performed to determine the K_d values by utilizing ternary solutions consisting of Nd^{3+}, Dy^{3+}, and Co^{2+} at equimolar concentrations between 0.075-1.2 mmol/L.

Figure 8a illustrates the relationship between the K_d values and the initial metal concentration. K_d values decrease as the initial metal concentration increases from 0.075 to 1.2 mmol/L. In particular, the maximum K_d values observed were 2716.01 mL/g for Nd^{3+}, 8600.8 mL/g for Dy^{3+}, and 159.92 mL/g for Co^{2+}. The variation of $\beta_{Nd^{3+}/Co^{2+}}$, $\beta_{Dy^{3+}/Co^{2+}}$, and $\beta_{Nd^{3+}/Dy^{3+}}$ as a function of initial concentration is shown in Figure 8b. It was inferred that am-TiP can selectively separate Nd^{3+} and Dy^{3+} from Co^{2+} across all concentrations examined. The maximum $\beta_{Nd^{3+}/Co^{2+}}$ value obtained was 20.04 at 0.15 mmol/L initial concentration, whereas the maximum $\beta_{Dy^{3+}/Co^{2+}}$ value was found to be 53.78 at 0.075 mmol/L. Due to the structural similarities between Nd^{3+} and Dy^{3+}, the selectivity coefficient values of Nd^{3+} over Dy^{3+} were below 2, indicating that individual separation conditions for Nd^{3+} and Dy^{3+} should be improved.
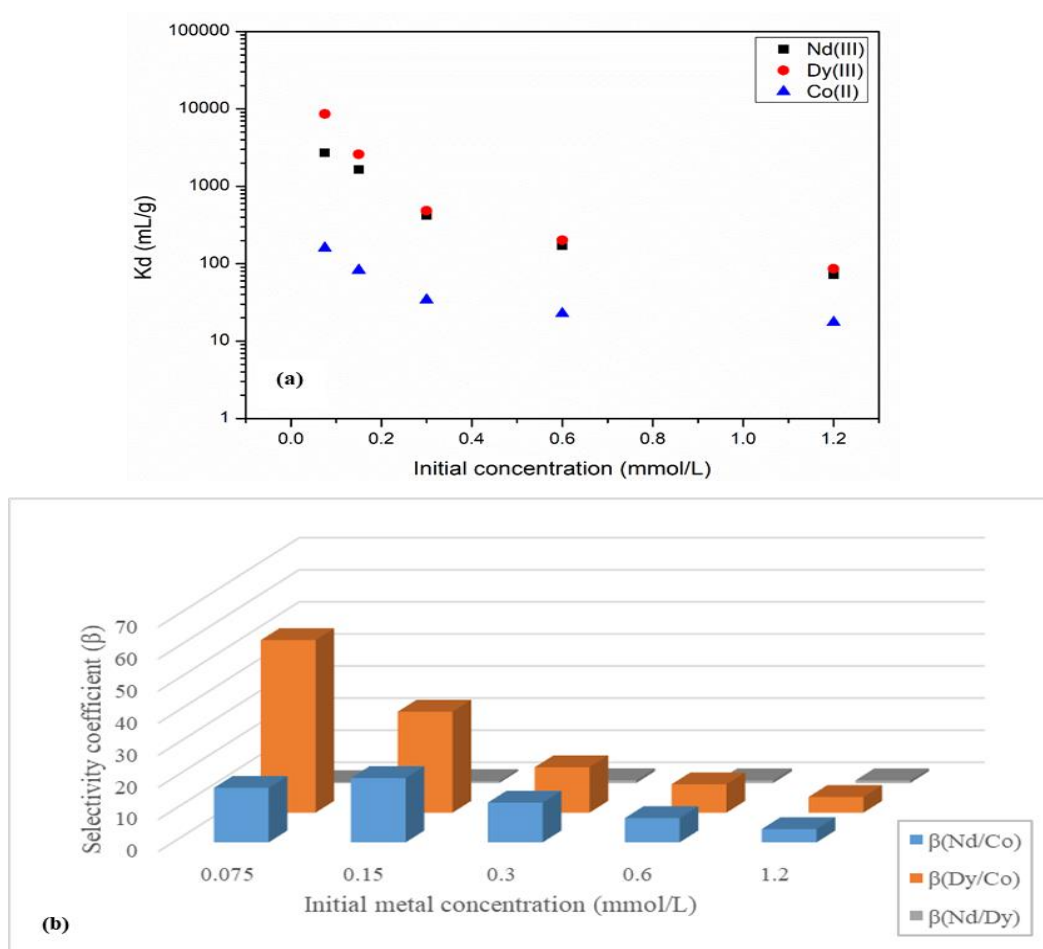
Figure 8: (a) K_d values and, (b) β values as a function of Nd and Dy concentration. (Experimental conditions: pH: 6; t: 60 min; T: 25 °C; m_{am-TiP}: 0.1 g; V: 30 mL)

Experimental runs were carried out to estimate the impact of initial pH on the sorption characteristics of am-TiP in mixed solutions. The tests were conducted using ternary solutions consisting of 0.3 mmol/L Nd^{3+}, Dy^{3+}, and Co^{2+} at pH values ranging from 2 to 6.

The impact of initial pH on the K_d values for Nd^{3+}, Dy^{3+}, and Co^{2+} is illustrated in Figure 9a. The metal uptake increased rapidly between pH 2 and 4, and the rate of increase decreased significantly after pH 4. At pH 6, the highest K_d values obtained

were 400.60, 479.55, and 43.42 mL/g for Nd^{3+}, Dy^{3+}, and Co^{2+} respectively.

Figure 9b exhibits the changes in $\beta_{Nd^{3+}/Co^{2+}}$, $\beta_{Dy^{3+}/Co^{2+}}$, and $\beta_{Nd^{3+}/Dy^{3+}}$ concerning the initial pH. The data indicate that am-TiP can selectively extract Nd^{3+} and Dy^{3+} from Co^{2+} across all pH values tested. The values of $\beta_{Nd^{3+}/Co^{2+}}$ and $\beta_{Dy^{3+}/Co^{2+}}$ exhibited an upward trend until pH 4, followed by a minor decrease beyond pH 4. At pH 3, the maximum $\beta_{Nd^{3+}/Co^{2+}}$ was recorded as 9.48, while at pH 4, the maximum $\beta_{Dy^{3+}/Co^{2+}}$ was found to be 12.59.
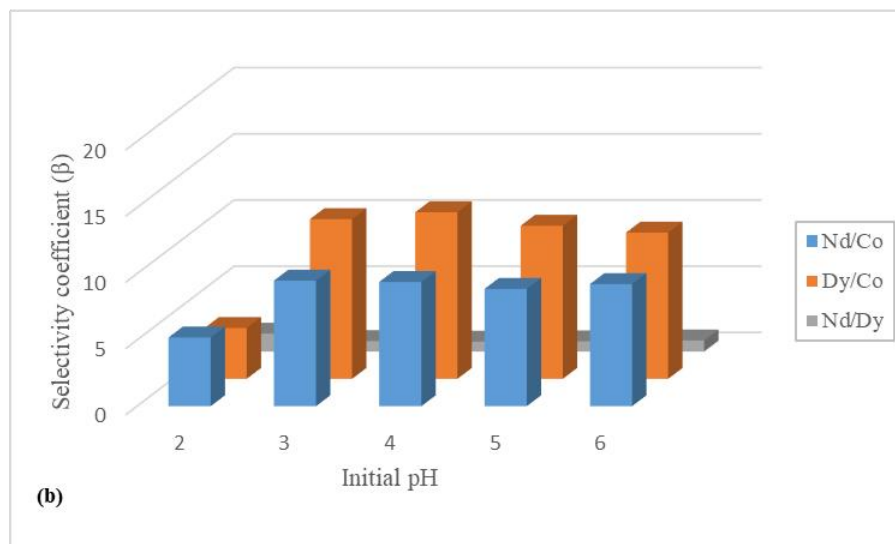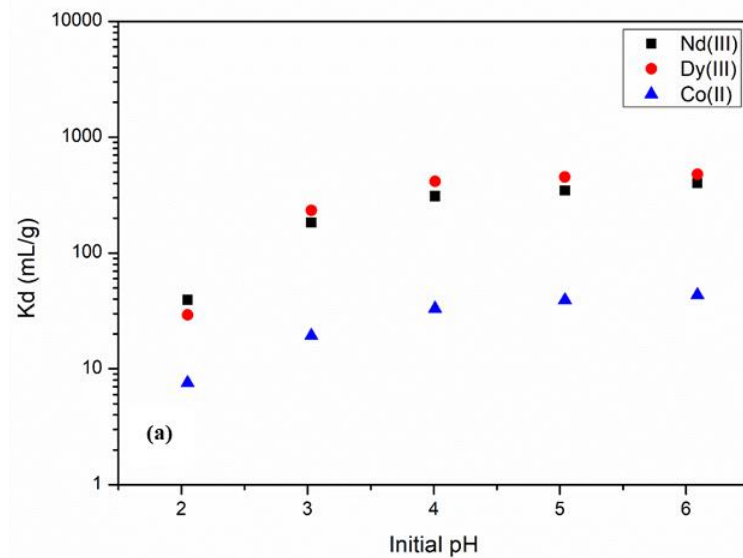
Figure 9: (a) K_d and (b) β values as a function of initial pH.
(Experimental conditions: C_i: 0.3 mmol/L; t: 60 min; T: 25 °C; m_{am-TiP}: 0.1 g; V: 30 mL)

3.4. Desorption Study and Reusability Tests
Effective control of metal-loaded sorbents after the sorption process is crucial for obtaining valuable data to design an efficient industrial operation. Hence, it is essential to perform desorption and re-use of the sorbents to recover the metals from wastewater streams in metal recovery processes (26). Based on the findings of the uptake

experiments, loading tests were conducted in the following conditions:

- Initial pH: 6
- Metal concentration: Equimolar (0.3 mmol/L) Nd^{3+}, Dy^{3+}, and Co^{2+}
- Contact time: 60 min
- Temperature: 25 °C
- Amount of am-TiP: 0.1 g

- Solution volume: 30 mL

After filtration, the metal-loaded am-TiP samples were washed with deionized water and allowed to dry at 50 °C for 24 h. In the next step, the metal-loaded sorbents were subjected to treatment with HNO_3, H_2SO_4, and HCl solutions of 0.1 and 1 mol/L concentrations for 60 min. Table 3 presents the data obtained from the desorption experiments carried out for Nd^{3+} and Dy^{3+}.

Table 3: Desorption percentage of Nd^{3+} and Dy^{3+} in different elution solutions.

Metal	0.1 mol/L HNO_3	1 mol/L HNO_3	0.1 mol/L H_2SO_4	1 mol/L H_2SO_4	0.1 mol/L HCl	1 mol/L HCl
Nd^{3+}	79.7	84.7	74.5	78.2	86.3	95.2
Dy^{3+}	81.4	85.1	76.8	80.6	88.8	97.4

The elution test showed that HCl was the most efficient acid. In a one-step batch process, a concentration of 1 mol/L hydrochloric acid was able to elute 57.6% of Nd^{3+} and 61.2% of Dy^{3+}. At the same concentration, the maximum desorption percentages obtained were 95.2% for Nd^{3+} and 97.4% for Dy^{3+}. The desorption, at both 0.1 and 1 mol/L concentrations, decreased in the following order: $HCl > HNO_3 > H_2SO_4$. Once the most efficient elution solution was determined (HCl-1 mol/L), the reusability of am-TiP was evaluated. A significant reduction in the sorption of Nd^{3+} and Dy^{3+} on am-TiP was observed after the third cycle, indicating a decrease in the reusability of the sorbent. The decline in the metal uptake could be attributed to the deformation of active sites on the surface due to repeated sorption-elution cycles or hydrolysis reactions taking place between the eluent and functional groups present on the sorbent surface.

4. CONCLUSION

In the study, am-TiP, a tetravalent metal phosphate compound, was synthesized and characterized for the selective separation of Nd^{3+} and Dy^{3+} ions from the leaching solutions of end-of-life Nd-Fe-B magnets. The structure was confirmed to contain phosphate groups through FTIR and EDS analyses.

Solution pH and metal concentration parameters have remarkable impacts on metal uptake from single-element solutions. Am-TiP was found to be efficient for Nd^{3+} and Dy^{3+} in the acidic region. The monolayer capacity of am-TiP was determined to be 40.16 mg/g for Nd^{3+} and 26.95 mg/g for Dy^{3+}.

If Co^{2+} ions are present in a solution, recovering Nd^{3+} and Dy^{3+} ions may be problematic. Thus, material selectivity is a crucial concern when choosing appropriate materials. Am-TiP was observed to be selective for Nd^{3+} and Dy^{3+} ions in a wide range of pH and concentration, in ternary solutions containing Nd^{3+}, Dy^{3+}, and Co^{2+} ions. For the separation of Nd^{3+}/Co^{2+} and Dy^{3+}/Co^{2+}, am-TiP has relatively high β values of 20.04 and 53.78, respectively. As anticipated, the comparable structure of Nd and Dy makes it challenging to separate them from each other. Using 1 mol/L HCl, the recovery of 95.2% Nd^{3+} and 97.4% Dy^{3+} from the loaded am-TiP was achieved. Am-TiP was found to be reusable for up to three regeneration cycles while maintaining its effectiveness.

The findings of the current study suggest that am-TiP exhibits comparatively good uptake capacities for Nd^{3+} and Dy^{3+}, as compared to previously reported data in the literature. Moreover, the material displays selectivity towards the separation of Nd^{3+} and Dy^{3+} ions from Co^{2+} ions in ternary solutions.

5. CONFLICT OF INTEREST

The author declares that there is no conflict of interest.

6. ACKNOWLEDGMENTS

7. REFERENCES

1. Gupta CK, Krishnamurthy N (Nagaiyar). Extractive metallurgy of rare earths. CRC Press; 2005. 484 p.

2. Maden Tetkik ve Arama Genel Müdürlüğü MTA Doğal Kaynaklar ve Ekonomi Bülteni Yıl: 2012 Sayı: 13 Ocak-Haziran.

3. Riaño S, Binnemans K. Extraction and separation of neodymium and dysprosium from used NdFeB magnets: An application of ionic liquids in solvent extraction towards the recycling of magnets. Green Chemistry. 2015 May 1;17(5):2931–42. Available from: <DOI>

4. Bogart JA, Lippincott CA, Carroll PJ, Schelter EJ. An Operationally Simple Method for Separating the Rare-Earth Elements Neodymium and Dysprosium. Angewandte Chemie. 2015 Jul 6;127(28):8340–3. Available from: <DOI>

5. Binnemans K, Jones PT, Blanpain B, Van Gerven T, Yang Y, Walton A, et al. Recycling of rare earths: A critical review. Journal of Cleaner Production. 2013;51:1-22. Available from: <DOI>

6. Yang Y, Walton A, Sheridan R, Guth K, Gauß R, Gutfleisch O, Buchert M, Steenari BM, Gerven TV, Jones PT, Binnemans K. REE recovery from end-of-life NdFeB permanent magnet scrap: A critical review. Journal of Sustainable Metallurgy. 2017;3:122-149. Available from: <DOI>

7. Tu YJ, Lo SC, You CF. Selective and fast recovery of neodymium from seawater by magnetic iron oxide Fe3O4. Chemical Engineering Journal. 2015 Feb 5;262:966–72. Available from: <DOI>

8. Durán SV, Lapo B, Meneses M, Sastre AM. Recovery of neodymium (III) from aqueous phase by chitosan-manganese-ferrite magnetic beads. Nanomaterials. 2020 Jun 1;10(6):1–12. Available from: <DOI>

9. Gok C. Neodymium and samarium recovery by magnetic nano-hydroxyapatite. Journal of Radioanalytical and Nuclear Chemistry. 2014;301(3):641–51. Available from: <DOI>

10. Saha D, Akkoyunlu SD, Thorpe R, Hensley DK, Chen J. Adsorptive recovery of neodymium and dysprosium in phosphorous functionalized nanoporous carbon. Journal of Environmental Chemical Engineering. 2017 Oct 1;5(5):4684–92. Available from: <DOI>

11. Komnitsas K, Zaharaki D, Bartzas G, Alevizos G. Adsorption of scandium and neodymium on biochar derived after low-temperature pyrolysis of sawdust. Minerals. 2017 Oct 26;7(10). Available from: <DOI>

12. Devi AP, Mishra PM. Biosorption of dysprosium (III) using raw and surface-modified bark powder of Mangifera indica: isotherm, kinetic and thermodynamic studies. Environmental Science and Pollution Research. 2019 Mar 8;26(7):6545–56. Available from: <DOI>

13. Aghayan H, Mahjoub AR, Khanchi AR. Samarium and dysprosium removal using 11-molybdo-vanadophosphoric acid supported on Zr modified mesoporous silica SBA-15. Chemical Engineering Journal. 2013 Jun 1;225:509–19. Available from: <DOI>

14. Avdibegović D, Zhang W, Xu J, Regadío M, Koivula R, Binnemans K. Selective ion-exchange separation of scandium(III) over iron(III) by crystalline A-zirconium phosphate platelets under acidic conditions. Separation and Purification Technology. 2019 May 15;215:81–90. Available from: <DOI>

15. Xu J, Wiikinkoski E, Koivula R, Zhang W, Ebin B, Harjula R. HF-Free Synthesis of α-Zirconium Phosphate and Its Use as Ion Exchanger for Separation of Nd(III) and Dy(III) from a Ternary Co–Nd–Dy System. Journal of Sustainable Metallurgy. 2017 Sep 1;3(3):646–58. Available from: <DOI>

16. Xu J, Koivula R, Zhang W, Wiikinkoski E, Hietala S, Harjula R. Separation of cobalt, neodymium and dysprosium using amorphous zirconium phosphate. Hydrometallurgy. 2018 Jan 1;175:170–8. Available from: <DOI>

17. Şentürk M, İnan S. Sorption and separation studies of Nd(III) and Dy(III) using amorphous tin(IV) phosphate. Chemical Papers. 2023 Jul 1;77(7):3835–45. Available from: <DOI>

18. Dutta A, Gupta D, Patra AK, Saha B, Bhaumik A. Synthesis of 5-hydroxymethylfurural from carbohydrates using large-pore mesoporous tin phosphate. ChemSusChem. 2014 Mar;7(3):925–33. Available from: <DOI>

19. de Vargas Briaõ G, da Silva MGC, Vieira MGA. Efficient and selective adsorption of neodymium on expanded vermiculite. Industrial & Engineering Chemistry Research. 2021;60(13):4962–74. Available from: <DOI>

20. Lewis A, Guéguen C. Using chemometric models to predict the biosorption of low levels of dysprosium by Euglena gracilis. Environmental Science and Pollution Research. 2022 Aug 1;29(39):58936–49. Available from: <DOI>

21. Langmuir I. The adsorption of gases on plane surfaces of glass, mica and platinum. Journal of the American Chemical Society. 1918;40(9):1361-1403. Available from: <DOI>

22. Freundlich H. Über die Adsorption in Lösungen. Zeitschrift für Physikalische Chemie. 1907;57U(1):385-470. Available from: <DOI>

23. Park HJ, Tavlarides LL. Adsorption of neodymium(III) from aqueous solutions using a phosphorus functionalized adsorbent. Industrial & Engineering Chemistry Research. 2010 Dec 15;49(24):12567–75. Available from: <DOI>

24. Zheng X, Liu E, Zhang F, Yan Y, Pan J. Efficient adsorption and separation of dysprosium from NdFeB magnets in an acidic system by ion imprinted mesoporous silica sealed in a dialysis bag. Green Chemistry. 2016;18(18):5031–40. Available from: <DOI>

25. Koochaki-Mohammadpour SMA, Torab-Mostaedi M, Talebizadeh-Rafsanjani A, Naderi-Behdani F. Adsorption Isotherm, Kinetic, Thermodynamic, and Desorption Studies of Lanthanum and Dysprosium on Oxidized Multiwalled Carbon Nanotubes. Journal of Dispersion Science and Technology. 2014 Feb;35(2):244–54. Available from: <DOI>

26. Kwon TN, Jeon C. Desorption and regeneration characteristics for previously adsorbed indium ions to phosphorylated sawdust. Environmental Engineering Research. 2012;17(2):65–7. Available from: <DOI>